EURODYN 2020
XI International Conference on Structural Dynamics
M. Papadrakakis, M. Fragiadakis, C. Papadimitriou (eds.)
Athens, Greece, 23–26 November 2020

SENSITIVITY OF DEFORMATION DEMANDS IN BUILDINGS TO MODELING ASSUMPTIONS IN NONLINEAR SEISMIC ANALYSIS

Jørgen R. Roven[1], **Emrah Erduran**[2] **and Amir M. Kaynia**[3]

[1]Rambøll
Hoffsveien 4, 0275 Oslo, Norway
e-mail: jrroven@protonmail.com

[2] Dept. of Civil Engineering and Building Technology, Oslo Metropolitan University
Pilestredet 35, 0166 Oslo, Norway
e-mail: emrah.erduran@oslomet.no

[3] Norwegian Geotechnical Institute
Sognsveien 72, N-0855 Oslo, Norway
e-mail: amir.m.kaynia@ngi.no

Keywords: Performance based design, Nonlinear seismic analysis, Displacement demands, Damage assessment, Numerical Models

Abstract.

Performance-based design principles rely heavily on the estimation of engineering demand parameters through nonlinear static or dynamic analysis. The increased focus on nonlinear analysis in recent and upcoming building codes calls for a detailed investigation into the limitations of these procedures. This is especially true for nonlinear dynamic analysis, which is often referred to as "exact" or "benchmark" solution. This article examines the sensitivity of nonlinear analysis results to the assumptions made in the modeling of nonlinear element behavior. To this end, a four-story reinforced concrete building designed according to the recent European standards is modeled in OpenSEES computational environment. Nonlinear element behavior is modeled using several approaches from lumped plasticity models to force-based and displacement-based elements with fiber sections using complex stress-strain curves. The results of nonlinear static and dynamic analysis reveal that the modeling assumptions have a significant effect on both displacement demands at the story and global level. More specifically, the curvature demands at the bottom of the ground story columns are very significantly affected by the modeling assumptions, particularly for diplacement- and force-based elements.

1 INTRODUCTION

Current seismic design procedures rely on elastic analysis where earthquake ground motions are simulated using equivalent lateral forces. On the other hand, ordinary structures that are designed using elastic analysis procedures are expected to be forced well beyond their elastic limit. The safety of these structures is ensured by prescriptive measures without actually evaluating their real performance. Performance based design procedures aim to provide a more transparent approach by evaluating the performance of the structure under different hazard levels. These methods rely heavily on estimation of engineering demand parameters such as total or plastic deformations through nonlinear static and dynamic analysis. As performance based design procedures are used more and more in seismic design, the numerical models become more complex. The assumptions used in the numerical modeling phase such as inelastic material behaviour, cyclic degradation and geometric nonlineareties can have severe implications for the results of an analysis [1–4]. For example, plastic rotations and curvatures of structural elements such as columns and beams are widely used for the assessment of the structural state in seismic design [2] and have been shown to be sensitive to the numerical parameters used in the analysis [5]. Although some studies [3, 5] have commented on the sensitivity of the engineering demand parameters to the numerical modeling assumptions, a quantitative documentation of this sensitivity is vital as the performance based design methods begin to find their way into seismic design codes.

The objective of this study is to investigate the effects of numerical modeling assumptions on the engineering demand parameters (EDPs) obtained from nonlinear static and dynamic analyses. Section curvatures, roof drifts and interstory drift ratios are chosen as the EDPs as these parameters have been documented to be well-correlated with structural damage. This will be done by conducting nonlinear static analyses (SPO) and nonlinear response history analyses (NRHA) on a reinforced concrete moment resisting frame (MRF) designed according to EN-1998-1 [6]. The analyses are performed using the open system for earthquake engineering simulation (OpenSees), which is an advanced computational tool frequently used in research.

2 THE ANALYZED STRUCTURE AND NUMERICAL MODELS

The analyzed structure is a four-story reinforced-concrete frame. It is symmetric about both horizontal axes with five bays in both directions. Due to the regularity of the building in plan, only one of the inner frames was modeled and used in the analysis. Figure 1 shows the elevation view of the of this frame. The structure was designed according to EN-1998:2004 [6] assuming moderate ductility level (DCM). All structural elements were designed for exposure class XC3, M60. The concrete quality was chosen as C30/37 and the thickness of cover concrete is 35mm for all elements. The reinforcement is of quality B500C with a modulus of elasticity of 200 GPa. The cross sections of the structural elements are summarized in Table 1.

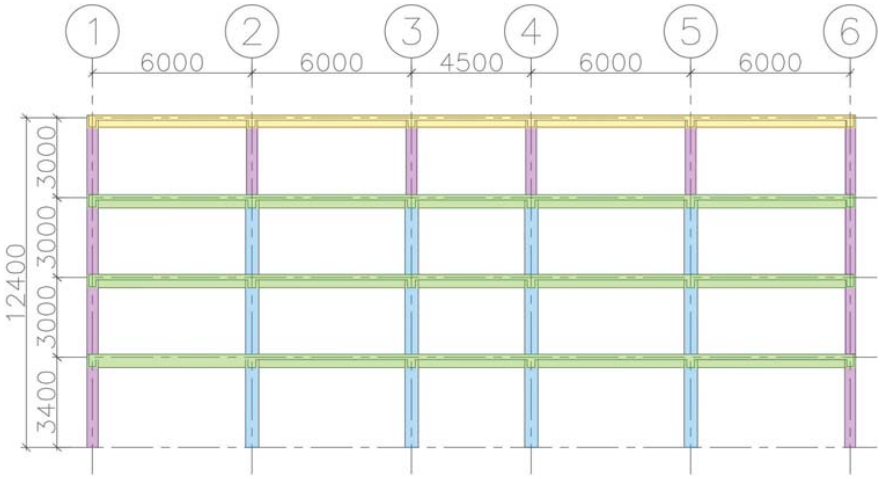

Figure 1: Elevation view of the analyzed frame (all measurements in mm)

Name	B [mm]	H [mm]	Color in Elevation View
Column 1	450	450	Pink
Column 2	500	500	Blue
Beam 1	300	500	Green
Beam 2	250	450	Yellow

Table 1: Cross sections of the structural elements of the frame shown in Figure 1.

The mass of the entire structure is 2 024 tons. The masses are lumped in their respective vertical level in nodes along axis 3. The natural periods for the first three modes were found to be 0.53, 0.17, and 0.10 seconds, respectively. Details of the structure can be found in [7]. For nonlinear response history analysis, damping of the system is modeled using 5% Rayleigh damping anchored at the $\omega_i = 0.707\omega_1$ (ω_1: the vibration frequency of the first mode) and $\omega_j = 31.4$ rad/s [8].

2.1 Structural Models

2.1.1 Element Models

All nonlinear analysis were carried out in the OpenSEES computational environment. Three types of structural element models were used in the analyses. The first element is a *force-based beam-column element* (FBE) that is based on the flexibility formulation and uses force interpolation functions for the variation of internal forces over the element length which represent the exact solution to the governing equations [9, 10]. The force-based approach relies on the equilibrium solution and, as such, even for nonlinear material response, FBE always satisfies the equilibrium conditions [11]. The inelastic properties are defined at integration points (IP) along the element, each contributing to the global inelasticity of the element [5]. The cross-sections of the elements have been modeled using fiber sections. Figure 2 illustrates a sample element with five integration points together with a sample fiber section where reinforcement, unconfined concrete and confined concrete fibers are depicted.

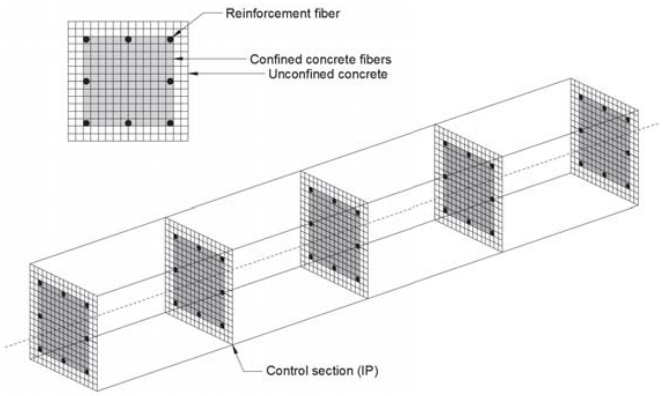

Figure 2: Illustration of the distributed plasticity model. One FE with five integration sections.

With regards to modeling softening behaviour, the stresses tend to localize in the most strained integration point (IP) of the most strained element [5]. As the number of integrations points are increased and the length of integration reduces, larger and larger rotations are required in the most strained IP for an element to produce same values of displacement, making the response nonobjective. Four to six IPs are necessary to accurately represent nonlinear material response and obtain an objective response [9].

The second element that was used in the analysis is the *displacement-based beam-column element* (DBE). This model is very similar to its force-based counterpart but uses the displacement formulation instead of the flexibility formulation. Despite their similarities, FBE and DBE cannot be modeled following the same approach. Most significantly, while the accuracy of the FBE can be improved by increasing either the number of integration points or the number of elements, the accuracy of the DBE can only be improved by increasing the number of elements.

The final element used in the present study is the *beam with hinges element* (BwH) which is also based on the flexibility formulation but the location and the weight of the integration points are predefined and based on the plastic-hinge formulation. This allows the users to specify plastic hinge lengths at the element ends. Two-point Gauss integration is used on the element interior while two-point Gauss-Radau integration is applied over lengths of $4Lp_I$ and $4Lp_J$ at the element ends [2, 12]. Figure 3 shows the underlying principles of the element together with the location of the integration points. The behaviour of the interior section can be modeled as linear elastic or inelastic; *e.g.* by using the fiber section shown in Figure 2. One of the most important parameters of BwH element is the plastic hinge length, l_p, which designates the part of the element where the nonlinear behavior is expected to occur, as the nonlinear behavior of the element depends, to a greater extent, to this parameter, especially if the interior of the element is modeled as linear elastic. There are different approaches to determine l_p, one of which is using empirical equations. One example can be found where Paulay and Priestly [13] provide an empirical formulation, and suggest that, for frame elements with normal proportions, this equation will lead to an approximate plastic hinge length of l_p = 0.5 h, where h is the depth of the cross section.

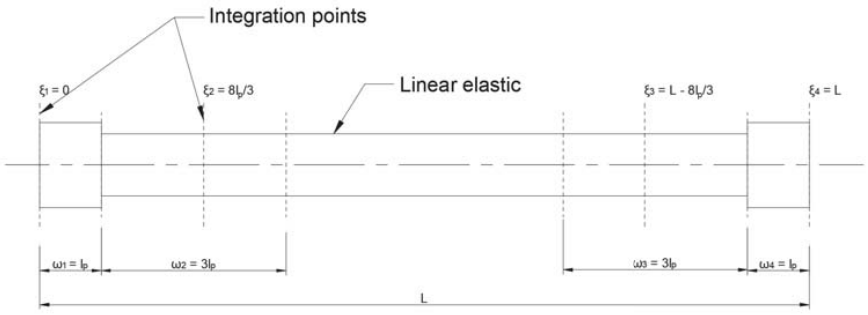

Figure 3: Beam with hinges element using the modified Gauss-Radeu integration rule.

2.1.2 Section and Material Models

All the cross-sections in the analysis were modeled using a fiber section as depicted in Figure 2. The material behavior at each fiber of the section is defined using a uniaxial stress-strain relationship. In order for a reliable nonlinear analysis, the concrete material model should be able to describe all material behaviours expected to occur before collapse during static and dynamic analyses. This includes, among other phenomena, strain softening and hardening, the effects of strain rates and confinement. To achieve this, the stress-straing model by Mander, Priestley and Park [14], which was based on Popovics model [15] and used extensively in literature (e.g. [2, 5, 16]), was used.

Two sets of parameters that were used for unconfined and confined concrete are presented in Table 2. The strain rate used in the calculations was 0.013 s^{-1}. The parameters shown in Table 2 were used as the input parameters for the CONCRETE04 material model in OpenSees. The reinforcement steel was modeled using the simplest model provided in OpenSees for steel, i.e STEEL01. The input parameters for this model were f_{yk} = 500 MPa, E_s = 200 GPa with a strain hardening ratio of b = 0.005.

Name	f_c	ϵ_c	ϵ_{cu}	E_c	ϵ_{ct}	ϵ_t
Unconfined concrete	-38.6	-0.00199	-0.0060	33.916	2.9	0.0855
Confined concrete nr.1	-47.9	-0.00420	-0.0142	-	-	-

Table 2: Concrete material parameters.

3 NUMERICAL ANALYSES

3.1 General

Nonlinear static analyses (NSA) and response history analyses (NRHA) were conducted using the elements described previously with different configurations. For the models using the DBE, each structural element was modeled using a different number of finite elements with two integration points. For the model using FBE such refinement is not necessary; instead the number of IPs per element has an effect and was thus varied. Similarly, only one finite element was used per structural element for the BwH elements. For the BwH element, the hinge length varied as well as the behavior of the interior section (elastic or inelastic). The different model configurations used in the analyses are summarized in Table 3. No NRHAs were performed using the DBE due to extremely long computational time and convergence issues.

Model	Configurations	Analyses
DBE	4, 8, 18 or 24 finite elements each using 2 IPs	NSA
FBE	One finite element using 2, 3, 4, 5, 6, 7 or 8 IPs	NSA and NRHA
BwH	l_p = {1.0h , 1.5h , 2.0h} with elastic interior	NSA and NRHA
BwH	l_p = {1.0h , 1.5h , 2.0h} with inelastic interior	NSA and NRHA

Table 3: Different model configurations

3.2 Nonlinear Static Analysis

NSA were performed to assess the behaviour of the structure and the different element formulations. The static pushover loads were applied at the nodes along axis 3 in a vertical pattern based on the eigenvectors of the first mode, making this a first-mode pushover analysis. P-δ effects were included in all analyses.

3.3 Nonlinear Response History Analysis

Nonlinear response history analyses were performed for a set of seven ground motion records for the different numerical models; in total 84 NRHAs. The ground motions records were selected for ground type C in EN 1998-1:2004 [6]. The ground motion records are listed in Table 4 with the corresponding parameters.

RSN	Name	Year	M_w	Rrap (km)	V_{s30} (m/sec)	PGA	SF
282	Trinidad	1980	7.2	76	312	0.22	2.32
720	Superstition Hills-02	1987	6.5	27	206	0.33	1.88
1003	Northridge-01	1994	6.7	27	309	0.64	0.76
1110	Kobe Japan	1995	6.9	25	256	0.25	1.67
4889	Chuetsu-Oki Japan	2007	6.8	33	315	0.37	1.29
5832	Iwate Japan	2010	6.9	31	248	0.40	1,121
6923	Darfield New Zealand	2010	7	31	255	0.47	0.99

Table 4: Ground motion records used for the analyses with the corresponding scale factors (SF).

The ground motions were scaled so that the spectral acceleration at the first natural period of the structure matches the elastic response spectrum defined in EN 1998 [6]. The scale factors used are also shown in Table 4. The scaled response spectra are plotted in Figure 4. The response of the structure is dominated by the first natural mode, hence scaling in this way is justified.

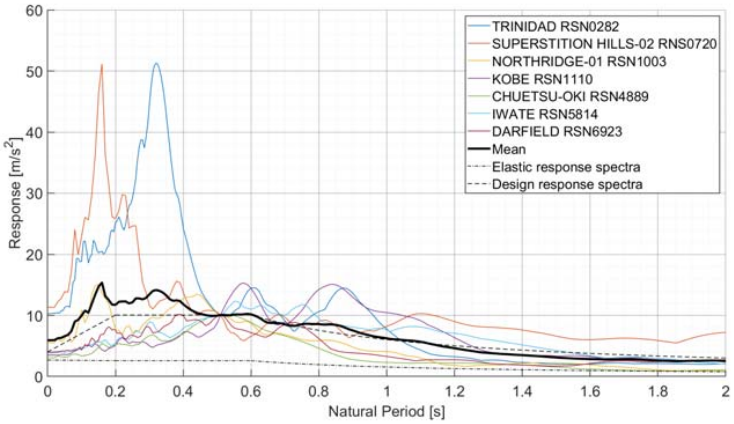

Figure 4: Response spectra scaled to match the elastic spectrum in EN-1998:2004 [6] at T_1.

4 RESULTS

4.1 Nonlinear Static Analysis

The capacity curves resulting from NSA for the different DBE models are shown in Figure 5. The results appear to converge to a stable solution as the number of FEs per member increases. As expected from the coarsely meshed models using DB elements, the base shear capacity of the structure is overestimated significantly for four- and eight-element models.

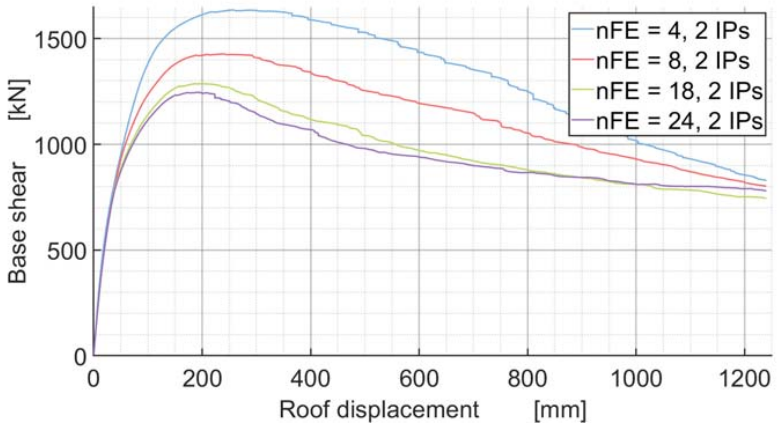

Figure 5: Base shear plotted against roof drift for different configurations of the DB model.

The response of the FBE model is nonobjective, i.e. as the number of IPs increases, the different curves do not converge towards a stable solution. Figure 6 presents capacity curves obtained from NSA using FBE. Figure 6 shows that increasing the number of IPs does not necessarily lead to a unique solution. Although the estimated maximum base shear load converges with increasing IP, the overall response, particularly, the immediate post-peak response shows discrepancies as the number of IPs increases. This can be attributed to the spread of nonlinearity over a larger part of the element as the number of integration points increases.

Comparing the computation time of NSA using DBE and FBE shows one of the significant disadvantages of DBE compared to the other elements, namely its poor efficiency. NSA using DBE with 18 FEs for each member provides a capacity curve quite similar to the one using FBE with 5 IPs per member. However, the computational time of the analysis with DBE is approximately five times that of the analysis with FBE.

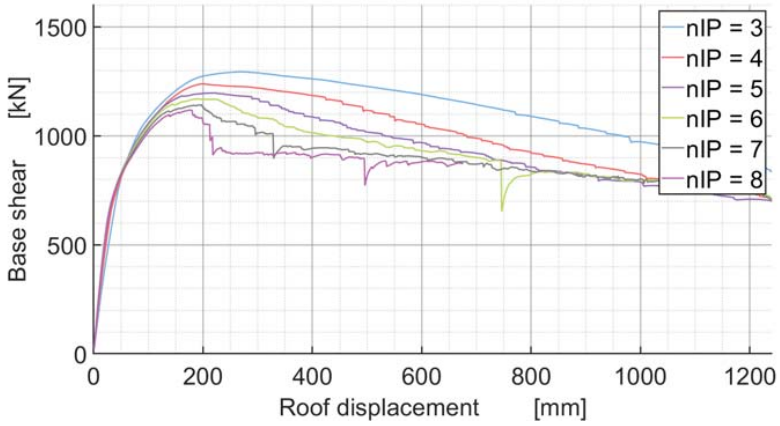

Figure 6: Base shear plotted against roof drift for different configurations of the FB model.

Using the BwH model, the models show similar responses for different plastic hinge lengths; see Figure 7. The stiffness of the structure immediately between first yielding (i.e. base shear around 500 kN) and the overall yielding is affected by the plastic hinge length if the element interior is modeled as elastic. When the element interior is inelastic, the capacity curves become virtually identical for different plastic hinge lengths. For the models where elements were defined with the inelastic fiber section in the interior, the response is generally softer. Note also that the model that used a hinge length of l_p = 2.0 h with an inelastic interior failed to converge at around 50 mm roof drift.

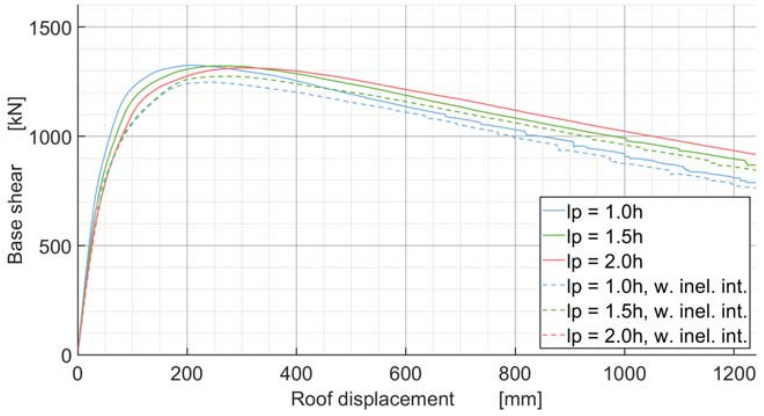

Figure 7: Base shear plotted against roof drift for different configurations of the BwH model.

One of the demand parameters that is strongly correlated with structural damage is the interstory drift ratio (IDR). Therefore, the effect of modeling assumptions on the IDR estimates

from NSA has been investigated. Figure 8 shows the IDRs for three different models at various roof drifts. From the IDR profiles at 2 and 4% roof drift, it can be seen that the three different models lead to very similar IDR estimates. As the roof drift increases, the DBE model starts displaying higher IDRs at the lower stories while the BwH leads to a higher estimate at the upper stories; Figure 8 (c).

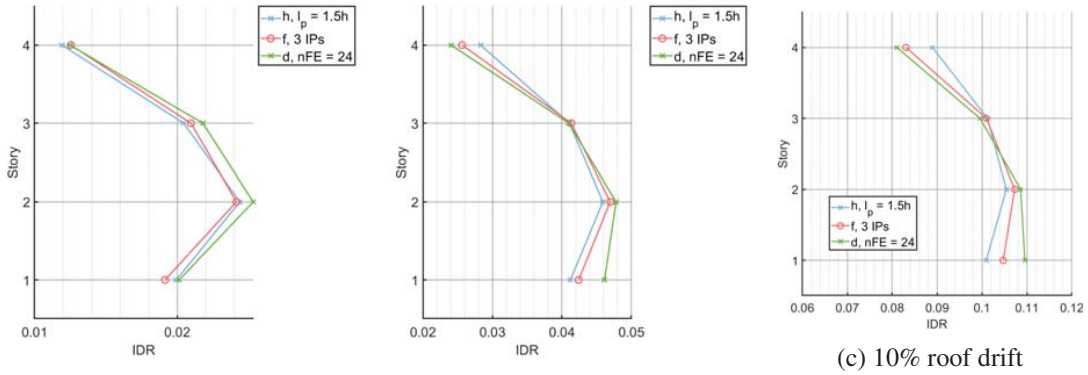

(a) 2% roof drift (b) 4% roof drift (c) 10% roof drift

Figure 8: IDRs for different element configurations at various roof drifts.

Curvature and curvature ductility at the element ends are often used as an indicator of damage at the element level. As such, variation of curvature estimates for different models can lead to a variation in the damage estimates. The curvature estimates at the bottom section of the ground story column in axis 3 from NSA is plotted against the roof drift in Figure 9. This plot illustrates how some of the model configurations give significantly different curvature estimates for a given roof drift even if the global demand estimates such as capacity curves and IDR estimates are rather similar. The most drastic variation is observed for FBE and DBE elements when the distance between the two integration points become rather short, either through increased number of IPs for FBE or through finer mesh for DBE.

Evaluating Figures 5 and 9 together presents a potential dilemma for use of displacement-based elements for nonlinear static analysis. More specifically, Figure 5 shows that in order to achieve a satisfactory capacity curve using DBEs, a fine mesh of 18 to 24 elements per member is necessary. However, using such a fine mesh leads to a potential problem that can have significant consequences as far as local behavior and damage estimates is concerned. As illustrated in Figure 9, using a very fine mesh, which is necessary to capture the global behavior satisfactorily, can lead to very high ductility demands for a given roof drift ratio compared to other models. These results are consistent with those found by Calabrese et al. [5] and others [17]; for softening behaviour, increasing the number of DB elements leads to nonobjective curvatures. The same issue can also be encountered for force-based elements when a high number of integration points is used as shown in Figure 9 and also reported by Calabrese et al. [5]. However, in case of FBE, the issue can be resolved by using less IPs, e.g. four or five, as these models produce very similar capacity curves compared to the model with 8 IPs.

With regards to the BwH model, Figure 9 shows results consistent with expectations. Since the characteristic length of the plastic hinge gets shorter, it must give higher values of curvature to produce the same displacements. As a result, the differences between the BwH model configurations are significant, although not as dramatic as FBE and DBEs with fine mesh.

The differences seen in curvature responses of these models can have direct implications for the estimated damage in the structural elements. It shows that when using a shorter hinge length or a finer mesh than the "correct" value, the level of damage may be greatly overestimated. Also, if a larger hinge length or a coarser mesh is used, the assessment may be unconservative.

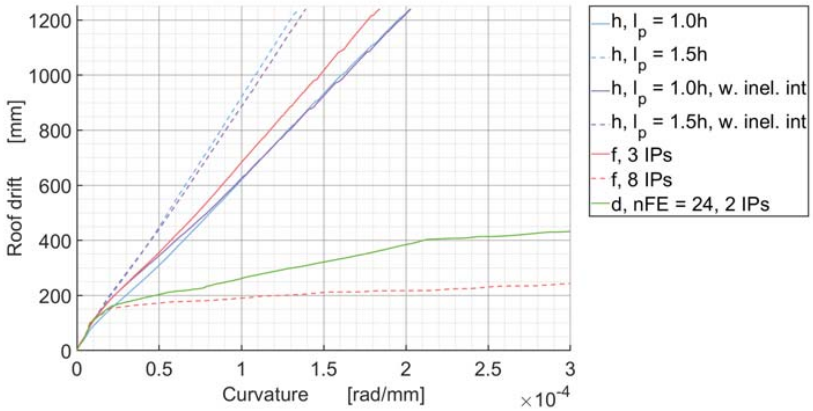

Figure 9: Roof drift plotted against the curvature in the monitored section.

4.2 Nonlinear Response History Analysis

The maximum interstory drift ratios obtained through NRHA for FBE, using different element configurations, are summarized in Figure 10. Here, it is seen that increasing the number of IPs beyond five appears to have little effect on the maximum IDR demands. Figures 11 and 12 shows the maximum IDRs for the BwH model, using elastic and inelastic interior, respectively. Both figures show that increasing the plastic hinge length for BwH elements lead to an increase in the maximum IDR demands for all ground motions.

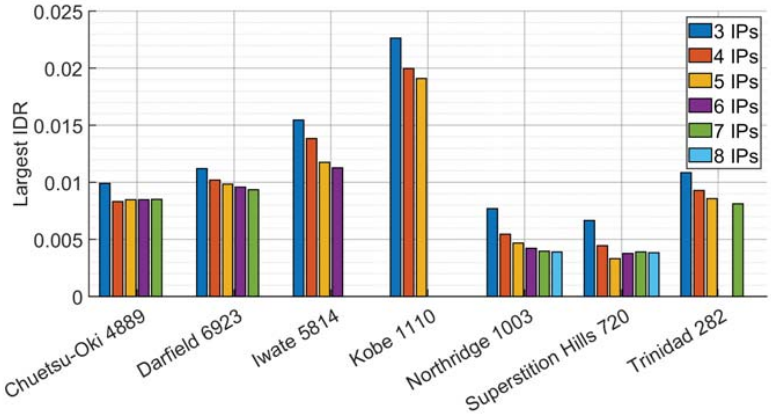

Figure 10: Maximum IDRs for the FB model.

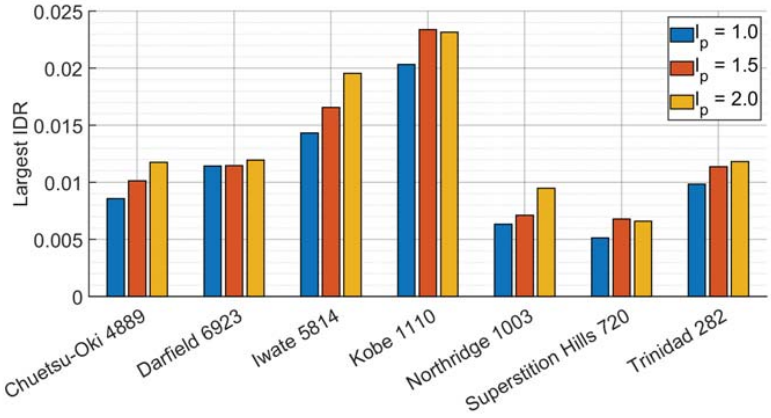

Figure 11: Maximum IDR for the BwH model using elastic interior.

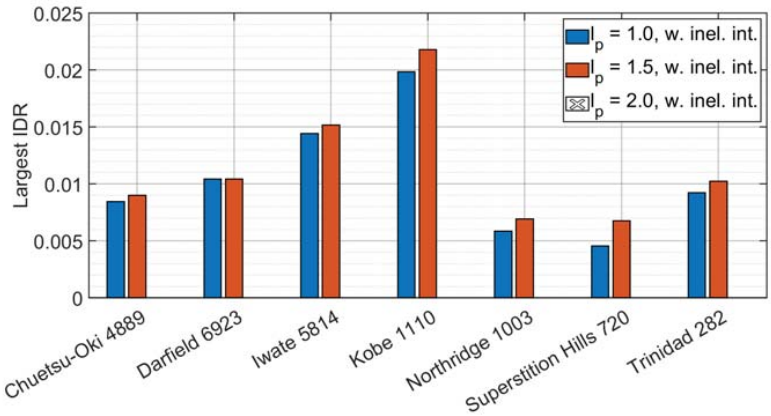

Figure 12: Maximum IDR for the BwH model using inelastic interior.

Figure 13 shows an overview of the mean value of the maximum roof drift ratios (RDR) and IDRs for the different model configurations. Across the various configurations, the trends shown for the RDRs and IDRs are very similar. For both parameters, it is evident that the peak responses decrease as the number of IPs increases for the FB model. For the BwH element, longer hinge lengths leads to larger peak values for both RDRs and IDRs. For elastic interiors, the peaks are somewhat larger when compared to the results from models using inelastic interiors.

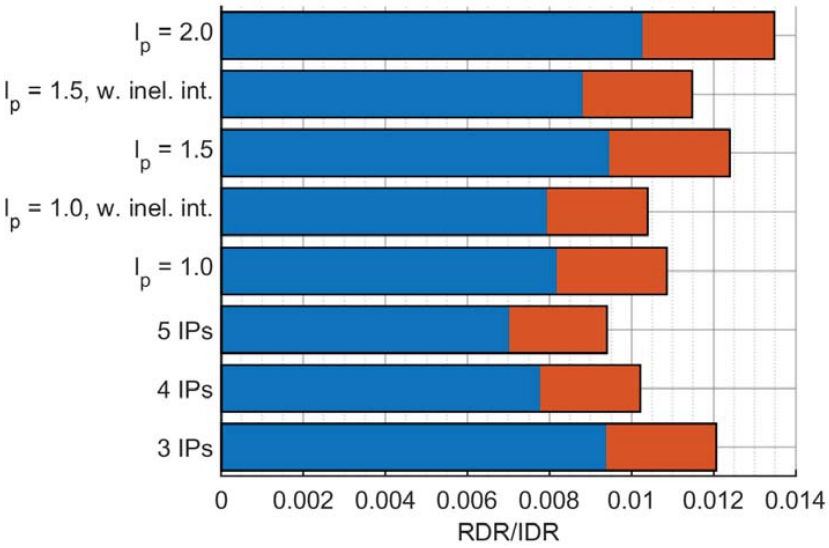

Figure 13: Mean values of RDRs and IDRs for the different numerical models. Blue bars represent RDRs while the values of the IDRs are represented by blue plus orange bars.

5 CONCLUSIONS

The objective of this study was to investigate the effect of modeling assumptions on deformation demand estimates of nonlinear static and dynamic analysis. This has been achieved through nonlinear static and dynamic analyses of a four-story reinforced concrete moment resisting frame using different model configurations. As a result of the analyses conducted, the following conclusions can be drawn:

- Use of displacement-based elements in nonlinear static analysis requires a fine mesh for a reliable capacity curve. Specifically, the base shear capacity of the structure can be significantly overestimated if less than 18 elements per member is used.
- Due to this requirement for a finer mesh, models created using displacement-based are computationally much more expensive compared to the models that use force-based elements.
- The modeling assumptions such as the number of integration points for forced-based element and the plastic hinge length for beam-with-hinges elements can have a significant effect on displacement demands such as interstory and roof drift ratios.
- The most significant impact of modeling assumptions have been observed for ductility estimates. For a given roof drift ratio, the ductility estimates can vary significantly from one model to another.
- The curvature estimates at the bottom of the ground story column from a displacement-based model with 24 elements per member are much higher compared to the other models. This is because, as the distance between the two element get smaller with finer mesh, very high curvatures at the exterior section can be required to achive the same roof displacement compared to other models with coarser mesh.

- Considering that a fine mesh is required in order to achieve a reliable capacity curve using displacement-based elements and the high curvature estimates for the same fine mesh, caution should be exercised when using this type of elements for nonlinear analysis.
- Force-based elements can also be susceptible to very high curvature estimates when a high number of integration points is chosen. To avoid this, the number of integration points has to be chosen carefully. The recommendation of using four to six IPs by Neuenhofer and Filippou [9] seems to provide satisfactory results at both global and local levels.
- The different types of elements available to an analyst, be it displacement-based, force-based or beam-with-hinges elements, have each their benefits as well as limitations and potential pitfalls. The different results show that an analyst must be able to assess what kind of phenomena are occurring in the numerical model in order to assess the objectivity of the results.
- More research that include a variety of structures and evaluate the sensitivity of more engineering demand parameters such as plastic rotations and hysteretic energy demands is necessary to enable the practitioners and researchers make informed decisions while developing nonlinear models.

References

[1] C. Zeris, D. Vamvatsikos, and P. Giannitsas. “Impact of Fe Modeling in the Seismic Performance Prediction of Existing Rc Buildings.” In: *ECCOMAS Thematic Conference on Computational Methods in Structural Dynamics and Earthquake Engineering*. Rethymno, 2007.

[2] M. H. Scott and G. L. Fenves. “Plastic Hinge Integration Methods for Force-Based Beam–Column Elements.” In: *Journal of Structural Engineering* 132.2 (2006), pp. 244–252.

[3] S. K. Kunnath and E. Erduran. *Pushover procedures for seismic assessment of buildings issues, limitations and future needs*. Tech. rep. Lisbon, Portugal, 2008, pp. 31–43.

[4] J. B. Mander. “Seismic Design of Bridge Piers.” Doctoral dissertation. University of Canterbury, 1983.

[5] A. Calabrese, J. P. Almeida, and R. Pinho. “Numerical Issues in Distributed Inelasticity Modeling of RC Frame Elements for Seismic Analysis.” In: *Journal of Earthquake Engineering* 14.sup1 (2010), pp. 38–68.

[6] Standard Norge. *NS-EN 1998-1 - Eurocode 8: Design of structures for earthquake resistance. Part 1: General rules, seismic actions and rules for buildings*. Lysaker, 2014.

[7] N. Øystad-Larsen, E. Erduran, and A. M. Kaynia. “Evaluation of effect of confinement on the collapse probability of reinforced concrete frames subjected to earthquakes.” In: *Procedia Engineering* 199 (2017), pp. 784–789.

[8] E. Erduran. “Evaluation of Rayleigh damping and its influence on engineering demand parameter estimates.” In: *Earthquake Engineering & Structural Dynamics* 41.14 (2012), pp. 1905–1919.

[9] A. Neuenhofer and F. C. Filippou. “Evaluation of Nonlinear Frame Finite-Element Models.” In: *Journal of Structural Engineering* 123.7 (1997), pp. 958–966.

[10] A. Neuenhofer and F. C. Filippou. “Geometrically Nonlinear Flexibility-Based Frame Finite Element.” In: *Journal of Structural Engineering* 124.6 (1998), pp. 704–711.

[11] E. Spacone, F. C. Filippou, and Fabio F. Taucer. “Fiber beam-column model for nonlinear analysis of R/C frames: Part II. Applications.” In: *Earthquake Engineering and Structural Dynamics* 25.7 (1996), pp. 727–742.

[12] OpenSees wiki. *Beam With Hinges Element*. 2006. URL: http://opensees.berkeley.edu/wiki/index.php/Beam_With_Hinges_Element (Cited 03/13/2018).

[13] T. Paulay and M. Priestley. *Seismic Design of Reinforced Concrete and Masonry Buildings*. 1st ed. New York: John Wiley and Sons, 1992.

[14] J. B. Mander, M. J. N. Priestley, and R Park. “Theoretical Stress-Strain Model for Confined Concrete.” In: *Journal of Structural Engineering* 114.8 (1988), pp. 1804–1826.

[15] S. Popovics. “A numerical approach to the complete stress-strain curve of concrete.” In: *Cement and Concrete Research* 3.5 (1973), pp. 583–599.

[16] D.-C. Feng and X.-D. Ren. “Enriched Force-Based Frame Element with Evolutionary Plastic Hinge.” In: *Journal of Structural Engineering* 143.10 (2017).

[17] J. Coleman and E. Spacone. “Localization Issues in Force-Based Frame Elements.” In: *Journal of Structural Engineering* 127.11 (2001), pp. 1257–1265.